

1 **Manganese incorporation in living (stained) benthic foraminiferal**
2 **shells: A bathymetric and in-sediment study in the Gulf of Lions**
3 **(NW Mediterranean).**

4 Shauna Ní Fhlaithearta¹, Christophe Fontanier^{2, 3, 4}, Frans Jorissen⁴, Aurélia Mouret⁴,
5 Adriana Dueñas-Bohórquez¹, Pierre Anschutz², Mattias B. Fricker⁵, Detlef Günther⁵,
6 Gert J. de Lange¹, Gert-Jan Reichart^{1, 6}

7

8 ¹ Faculty of Geosciences, Utrecht University, Utrecht, The Netherlands.

9 ² EPOC, UMR CNRS 5805, University of Bordeaux, Pessac, France

10 ³ FORAM, Foraminiferal Study Group, F-29200, Brest, France

11 ⁴ Université d'Angers, LPG-BIAF, UMR CNRS 6112, 49045 Angers Cedex, France

12 ⁵ Laboratory of Inorganic Chemistry, ETH Zurich, 8093 Zurich, Switzerland.

13 ⁶ Royal NIOZ, Texel, The Netherlands

14

15 Corresponding author: S. Ní Fhlaithearta, s.ni.fhlaithearta@gmail.com

16 Keywords: Benthic foraminifera, minor/trace metals, calibration study, Gulf of Lions, Mn/Ca

17

18 **Abstract**

19 Manganese geochemistry in deep-sea sediments is known to vary greatly over the first
20 few centimeters, which overlaps with the in-sediment depth habitats of several benthic
21 foraminiferal species. Here we investigated manganese incorporation in benthic
22 foraminiferal shell carbonate across a 6-station depth transect in the Gulf of Lions, NW
23 Mediterranean to unravel the impacts of foraminiferal ecology and Mn pore water
24 geochemistry. Over this transect water depth increases from 350 to 1987 m, while
25 temperature (~13°C) and salinity (~38.5) remained relatively constant. Manganese
26 concentrations in the tests of living (Rose Bengal stained) benthic foraminiferal
27 specimens of *Hoeglundina elegans*, *Melonis barleeanus*, *Uvigerina mediterranea*,
28 *Uvigerina peregrina* were measured using laser ablation inductively coupled mass
29 spectrometry (laser ablation ICP-MS). Pore water manganese concentrations show a
30 decrease from shallow to deeper waters, which corresponds to a generally decreasing

31 organic matter flux with water depth. Differences in organic matter loading at the
32 sediment water interface affects oxygen penetration depth into the sediment and hence
33 Mn pore water profiles. Mn/Ca values for the investigated foraminiferal species reflect
34 pore water geochemistry and species-specific microhabitat in the sediment. The
35 observed degree of variability within a single species is in-line with know ranges in
36 depth habitat and gradients in redox conditions. Both Mn/Ca ratio and inter-specific
37 variability hence reflect past Mn cycling and related early diagenetic processes within
38 the sediment, making this a potential tool for bottom-water oxygenation and organic-
39 matter fluxes. Dynamics of both in-sediment foraminiferal depth habitats and Mn
40 cycling, however, limit the application of such a proxy to settings with relatively stable
41 environmental conditions.

42

43 **1. Introduction**

44

45 Reconstructing past climate and environmental change largely depends on so-called
46 proxies. These proxies relate measurable variables in the geological record to target
47 parameters, such as e.g. temperature, biological productivity and bottom water
48 oxygenation. The carbonate shells of unicellular protists, foraminifera, are one of the
49 most utilized signal carriers for reconstructing past environments. Both the census data
50 of foraminifera and the geochemical composition of the shells are used in this context.
51 The geochemical composition of the shells is investigated for their stable isotopic
52 composition as well as for their trace and minor element incorporation. Both pelagic
53 and bottom water conditions are reconstructed this way, using planktonic and benthic
54 foraminiferal species respectively.

55

56 Most existing calibrations of trace element uptake in foraminiferal test
carbonate are based on comparing their composition with bottom water conditions

57 (Elderfield et al., 2006; Nürnberg et al., 1996; Yu and Elderfield, 2007). Many benthic
58 foraminiferal species live, however, within the sediment and precipitate their calcium
59 carbonate test in contact with pore water. As a result, the trace metal composition of
60 pore water exerts a control on the uptake of trace metals in their test. This effectively
61 links benthic foraminiferal microhabitat preference and pore water chemistry. On the
62 one hand, this creates complications when using foraminiferal trace metal ratios for
63 reconstructing bottom water conditions, whereas on the other hand, it offers the
64 possibility to develop proxies of pore water chemistry in the past.

65 Linking foraminiferal test chemistry with pore water chemistry requires in-
66 depth knowledge of, 1) how early diagenesis in sediments affects pore water chemistry,
67 2) the habitat preference of the foraminiferal species, 3) foraminiferal migration (and
68 the depth at which they calcify) within the uppermost sediment layer. In principle, the
69 chemical composition of living (stained) benthic foraminifera will reflect all these
70 processes.

71 For many elements an important inter-specific difference in uptake of trace
72 metals has been observed (Hintz et al., 2006; Wit et al., 2012; Barras et al., 2018), a so-
73 called vital effect. This implies that in addition to ecology and pore water geochemistry,
74 trace metal partitioning also needs to be taken into consideration. This requires a
75 comparative study between locations where all three of these aspects have been
76 quantified.

77 Reconstructing past pore water trace metal profiles is important since it provides
78 valuable information on organic carbon degradation and recycling of nutrients at the
79 seafloor (Van Cappellen and Wang, 1996; De Lange, 1986). Such diagenetically
80 controlled trace metal profiles are used in quantitative models constraining oceanic

81 carbon fluxes and burial (Wang and Van Cappellen, 1996). Knowledge of such profiles
82 in the past could thus help to reconstruct past carbon cycles.

83 Benthic foraminiferal species have a specific preference for their depth-habitat
84 (Jorissen et al., 1995). Some benthic foraminiferal species are limited to a very narrow
85 environmental in-sediment range, for example, along redox fronts, whereas others have
86 a wider distribution, thriving under variable conditions and consequently occupy a
87 broader niche. These differences in depth-habitat preferences could be related to the
88 presence of different types of metabolism (Koho et al., 2011; Risgaard-Petersen et al.,
89 2006). As such, trace metal profiles and foraminiferal in-sediment depth habitat can be
90 related, such as recently proposed in a conceptual (TROXCHEM³) model for the redox
91 sensitive element, manganese, by Koho et al. (2015). Studying the interplay between
92 benthic foraminiferal habitat preference and incorporation of redox-sensitive trace
93 elements is key to verifying such models.

94 Studying manganese bound in foraminiferal shell carbonate lies at the
95 intersection of foraminiferal ecology and early diagenesis in sediments. Manganese is
96 a redox sensitive element and exists as Mn-(hydr)oxides in the presence of oxygen. As
97 oxygen concentrations in the sediment decreases due to ongoing organic matter
98 remineralization, Mn-(hydr)oxides are reduced to aqueous Mn²⁺, (Froelich et al., 1979).
99 Manganese in sediments cycles continuously between solid and aqueous state as a result
100 of upward diffusion of Mn²⁺ and consequent remineralization to Mn-(hydr)oxides.
101 Hence proxy studies must account for both ecological controls, like foraminiferal
102 habitat preference, as well as geochemical controls like oxygen concentrations and
103 organic matter loading (Glock et al., 2012; Groeneveld and Filipsson, 2013; Koho et
104 al., 2015, 2017; McKay et al., 2015; Reichart et al., 2003). Notably, both benthic
105 foraminifera and trace metal geochemistry react to organic matter recycling and bottom

106 water oxygenation (Jorissen et al., 1995). This implies that locations with contrasting
107 conditions, both low and high bottom-water oxygenation as well as low and high
108 productivity, are required for testing. Whereas most of these studies focused on the role
109 of bottom water oxygenation in relatively oxygen poor settings, here we focus on the
110 well-oxygenated western Mediterranean.

111 In this study we combine pore water geochemistry, foraminiferal habitat
112 preference and test geochemistry in an area characterized by well-oxygenated bottom
113 water conditions and average productivity. Results are compared with earlier studies
114 from high productivity regimes and low-oxygen conditions at the sediment-water
115 interface (e.g. Arabian Sea, Koho et al., 2015 and Mediterranean sapropel deposition,
116 Ní Fhlaithearta et al., 2010). Specifically, we investigate the link between manganese
117 incorporation and benthic foraminiferal ecology and compare this to the recently
118 proposed TROXCHEM³ model (Koho et al., 2015). Four species of living (stained)
119 foraminifera were sampled along a 6-station bathymetric transect in the Gulf of Lions,
120 NW Mediterranean. Individuals were picked from a series of in-sediment depths and
121 analyzed by laser ablation ICP-MS, enabling multiple analyses of single specimens.

122

123 **2. Material and methods**

124

125 **2.1 Study area and sediment sampling**

126 Cores were collected with a classical Barnett multicorer (Barnett et al. 1984) at 6
127 stations in the Gulf of Lions (NW Mediterranean) during the August-September 2006
128 BEHEMOTH cruise (Fig. 1, Table 1). The 6 stations describe a bathymetric transect
129 from 350m to 1987m depth. The shallowest site, station F, is bathed in Mediterranean
130 Intermediate Water (MIW). Stations E (552 m) and D (745 m) are positioned at the

131 transition of MIW and Western Mediterranean Deep Water (WMDW). Stations C (980
132 m), B (1488 m) and A (1987 m) are bathed by the WMDW. Bottom water temperature
133 is stable through the part of the water column studied here ($\sim 13.1^{\circ}\text{C}$) (Xavier Durrieu
134 de Madron, pers. com.). Salinity ranges between 38.4 and 38.5. The multicorer allowed
135 sampling of the first decimeters of the sediment, the overlying bottom waters, and an
136 undisturbed sediment-water interface. Cores were sliced for foraminiferal studies with
137 a 0.5-cm resolution down to 4 cm, followed by 1 cm slices down to 10 cm depth.
138 Sediments were put in an ethanol-Rose Bengal mixture (95% ethanol with 1g/l Rose
139 Bengal), in order to identify living (stained) specimens. For more detailed information
140 about methods, please consult Fontanier et al., (2008).

141

142

143 **2.2 Pore water geochemistry**

144 Sediment sampling for pore water extraction was carried out under an inert atmosphere
145 (N_2). Hereafter, samples were centrifuged at 3500 rpm for 20 min. The supernatant was
146 filtered and acidified (HNO_3 *s.p.*) for analyzing dissolved metals. Dissolved Mn
147 concentrations were determined with flame atomic absorption spectrometry (Perkin
148 Elmer AA 300). Precision for this method is $\pm 5\%$. A pore water subsample was also
149 analyzed for Mn using ICP-MS (Agilent 7500 Series). Relative precision for this
150 method is 3%. Total alkalinity of pore water was measured at Utrecht University using
151 an automated titrator (702 SM Titrino, Metrohm) making Gran plots. Dissolved
152 Inorganic Carbon (DIC) was measured using a Dissolved Carbon Analyser (Shimadzu,
153 Model TOC-5050A). Carbonate ion concentrations were calculated using the CO2SYS
154 software (version 01.05; Lewis and Wallace, 1998). Analytical uncertainty for the
155 alkalinity is about 10 μeq , relative standard deviation for the DIC analyses is 0.8%.

156 Oxygen concentration profiles were determined using Clark-type
157 microelectrodes (Unisense©, Denmark). Labile organic matter was derived from the
158 sum of lipids, amino acids and sugars measured in the top cm of sediment; for details,
159 see Fontanier et al., 2008.

160

161 **2.3 Foraminiferal trace metal geochemistry**

162 Foraminiferal trace element concentrations were determined using two laser ablation
163 ICP-MS systems. Prior to laser ablation, all samples were gently cleaned in methanol
164 (x1) and UHQ water (x4). Between each rinse, the samples were placed in a sonic bath
165 for several seconds to thoroughly clean the tests. Benthic foraminifera from 745 m
166 (station D), 980 m (station C), 1488 m (station B) and 1987 m (station A) were
167 measured at Utrecht University using a deep UV (193nm) ArF excimer laser (Lambda
168 Physik) with GeoLas 200Q optics. Ablation was performed at a pulse repetition rate of
169 10 Hz, and energy density of 1.4 J/cm², with a crater size of 80µm. Ablated particles
170 were measured by a quadrupole ICP-MS (Micromass Platform) equipped with a
171 collision and reaction cell. Such a collision and reaction cell improves carbonate
172 analyses by eliminating interferences on mass 44. Scanned masses included ²⁴Mg, ²⁶Mg,
173 ²⁷Al, ⁴²Ca, ⁴³Ca, ⁵⁵Mn, ⁸⁸Sr, ¹³⁷Ba, ¹³⁸Ba, ²⁰⁸Pb. Benthic foraminifera from stations F (350
174 m) and E (552 m) were analyzed at ETH-Zurich (due to laboratory renovations at
175 Utrecht University). The laser type and ablation parameters were identical to those
176 detailed above. The ablated particles were measured using a quadrupole ICP-MS
177 (ELAN 6100 DRC, Perkin-Elmer). In both cases, calibration was performed using an
178 international standard (NIST610) with Ca as an internal standard (Jochum et al. 2011).
179 The same masses as measured in Utrecht were monitored, in addition to ⁷Li, ²³Na, ⁴⁷Ti,
180 ⁶⁰Ni, ⁶¹Ni and ⁸⁹Y. Inter-laboratory compatibility was monitored using a matrix-matched

181 calcite standard. For Mn this standard showed a precision better than 3% over all
182 analyses, at ETH and UU, and with an offset of less than 5% from an off line determined
183 (solution ICP-AES) concentration analyzing discrete sub-samples. The matrix matched
184 standard is routinely included in the analyses and has been monitored since 2010
185 (Duenas Bohorquez et al., 2011).

186 Analytical error (equivalent to 1 sigma), based on repeated measurement of an
187 external standard, was <5% for reported elements. Each laser ablation measurement
188 was screened for contamination by monitoring Al and Pb. On encountering surface
189 contamination, the data integration interval was adjusted to exclude any Al or Pb
190 enrichment. Cross-plots between Al and Pb versus Mn showed that they are unrelated,
191 confirming accuracy of the integrations.

192 During the laser ablation analyses the different trace elements were monitored
193 with respect to time, thus representing a cross section of the test wall. This allows not
194 only quantification of the different trace metals of interest, but also to observe
195 variability within individual tests. Each species has a distinct test-wall thickness,
196 permitting the study of intra-test variability. A typical ablation profile for *H. elegans* is
197 shown in Fig. 2.

198

199 **2.4 Analyses of manganese in foraminiferal tests**

200 Contamination and presence of secondary Mn-rich coatings on benthic foraminiferal
201 tests has been a longstanding challenge in trace metal analyses of benthic foraminifera
202 (Boyle 1983, Lea and Boyle 1989). In this study the trace metal data are based
203 exclusively on living (Rose Bengal stained) foraminifera, which effectively rules out
204 the impact of Mn-rich coatings on trace metal concentrations. At the time of
205 sampling, the collected tests were still enveloped by foraminiferal cytoplasm,

206 preventing the formation of extraneous inorganic precipitates. Although benthic
207 foraminifera live within the sediment, their test is physically separated from the
208 environment as they are enveloped in an organic sheath (Ní Fhlaithearta et al., 2013).
209 In case a recently deceased foraminifer was mistakenly analyzed (still with sufficient
210 protoplasm to stain with Rose Bengal) the Mn oxide would not only have had limited
211 time to develop, but it would also show up as a Mn spike at the start of a laser ablation
212 profile. The ablation profiles confirm that no Mn-rich phases are present at the test
213 surfaces (Fig. 2).

214 Comparing LA-ICP-MS data with traditional solution analyses for foraminiferal
215 Mg/Ca values showed that data are directly comparable (Rosenthal et al., 2011). Also
216 for trace metals such as Ni²⁺, Cu²⁺ and Mn²⁺, cross-calibration of LA-ICP-MS and
217 micro-XRF shows those analytical results are robust (Munsel et al., 2010).

218

219 **2.5 Benthic foraminiferal Mn/Ca**

220 Manganese incorporation in benthic foraminiferal test carbonate was analyzed from 4
221 different species (*Hoeglundina elegans*, *Melonis barleeanus*, *Uvigerina mediterranea*,
222 *Uvigerina peregrina*), from 6 coring sites, for up to 9 depths in the sediment. Sample
223 coverage for all stations is described in Table 2. Descriptive statistics are presented in
224 Table 3.

225 From the largest taxon, *Uvigerina mediterranea*, 3-4 analyses were routinely carried
226 out per test, and no trend in Mn/Ca values was seen in consecutive growth stages. From
227 the other species two analyses were performed per test. The resolution of the ablation
228 profiles themselves does not allow quantifying changes in trace metals within the test
229 wall. Still, comparing the data within individual ablation profiles shows that the
230 intratest variability is generally limited for Mn (Table 4). As the ablation profiles target

231 one chamber mostly, this does not include the full potential range. Comparing different
232 ablation profiles between chambers in a single shell would circumvent this, but this data
233 is somewhat limited.

234 Boxplots are used to describe the range of Mn/Ca values and how the distribution,
235 median, average and skewness compares between species. All ICP-MS measurements
236 are included, and as such represent both intra- and inter-individual variation.

237

238 **3. Results**

239 **3.1 Pore water data**

240 Pore water dissolved manganese (Mn^{2+}) concentrations were measured at all six
241 stations. Manganese concentrations increase below the oxygen penetration depth at
242 stations C and D (Fig. 3), with the highest in-sediment Mn^{2+} concentrations reached at
243 station D. At stations E and F manganese concentrations remain low after crossing the
244 oxygen penetration depth. At stations A and B the oxygen penetration depth and
245 $\text{MnO}_2/\text{Mn}^{2+}$ redox boundary are deeper than 10 cm's. Dissolved inorganic carbon (DIC)
246 and total alkalinity (TA), were measured at stations E, C and B (Fig. 4). At stations D,
247 C and E, DIC concentrations in the top 10 cm have a similar range (2350-2700
248 $\mu\text{mol/kg}$). The DIC profile at station B has a narrower range, ranging from 2400-2550
249 $\mu\text{mol/kg}$. Total alkalinity values range from 3242 $\mu\text{mol/kg}$ at station E to a minimum
250 of 2774 at station B. Carbonate ion concentrations [CO_3^{2-}] were derived based on TA
251 and DIC values. The [CO_3^{2-}] profiles were relatively similar (Fig. 4) for stations E and
252 C and B. Values for all three stations ranged from a maximum of 419 $\mu\text{mol/kg}$ at station
253 E to a minimum of 192 $\mu\text{mol/kg}$ at station C (Fig. 4).

254 **3.2 Mn/Ca data**

255 **3.2.1 Intra-individual variability**

256 For most species some Mn/Ca analyses were below detection limit, except for *M.*
257 *barleeanus*, which contained measurable quantities of Mn in all shells analyzed. This
258 was most evident for *H. elegans*, where all but three Mn/Ca measurements were below
259 detection limit (dl). *Uvigerina peregrina* had a wider range of Mn/Ca values than *U.*
260 *mediterranea*. *Melonis barleeanus* exhibited the largest range of Mn/Ca values of the
261 four studied species (Fig. 5). For all species, except *H. elegans*, values are somewhat
262 skewed towards higher values.

263

264 **3.2.3 Foraminiferal Mn/Ca variation across a depth transect**

265 A trend of decreasing manganese incorporation with increasing water depth (350-1987
266 m) is most clearly visible in *M. barleeanus* (Fig. 6), except that the maximum values
267 are observed at station E at 552 m. *Melonis barleeanus* shows the highest Mn/Ca values
268 and the largest Mn/Ca variability. Station E registers the broadest Mn/Ca variability,
269 which decreases with increasing water depth. *U. peregrina* also exhibits the largest
270 variability in Mn/Ca values at station E. For *U. peregrina*, Mn²⁺ incorporation decreases
271 from 350 m to 1987 m, except for station D (745 m), where Mn/Ca values (between the
272 10 – 90th percentile) are approximately equivalent to those at station A (350 m; Fig. 6).
273 For *U. mediterranea* a trend of decreasing Mn incorporation with increasing depth is
274 found in specimens of *U. mediterranea* from the sediments at 552, 745 and 980 m. The
275 highest values are reached at the shallowest station (350 m). Station E is also marked
276 by the highest minimum Mn/Ca values for *U. mediterranea*. At station A only two *U.*
277 *mediterranea* measurements are above the detection limit. *Hoeglundina elegans* shells
278 from three stations (350 m, 1488 m and 1987 m) were analyzed, however, all but three

279 measurements were below detection limit (Fig. 6). These slightly elevated values were
280 recorded at the shallowest station (station F). These Mn/Ca values are still very low
281 compared to ranges in Mn/Ca values observed for the other species (Fig. 6).

282 Variability in Mn/Ca increases together with the overall Mn/Ca concentration
283 within benthic foraminiferal species (Table 4). This suggests that even at those stations
284 and depth levels where the highest Mn concentrations are recorded, individuals with
285 relatively low amounts of Mn in their calcitic test were found. Comparing relative
286 standard deviations, as a measure for the inter-specimen variability, for the different
287 stations and species suggests that with increasing Mn concentration for *M. barleeanus*
288 and *U. mediterranea* variability increases, whereas for *U. peregrina* it decreases.

289

290 **3.2.4 In-sediment variation**

291 For most species Mn/Ca values are more or less constant with in-sediment depth (Fig.
292 3). However, *M. barleeanus* shows increasing Mn/Ca values with in-sediment depth.
293 This is most apparent at the shallowest station (station F - 350 m) (Fig. 3d).

294

295 **4. Discussion**

296

297 Incorporation of Mn in benthic foraminiferal carbonate depends both on foraminiferal
298 ecology and early diagenesis in sediments. Although other factors such as temperature,
299 sea water carbonate chemistry, growth rate etc., might also affect the uptake of Mn in
300 the shell carbonate (Koho et al., 2017), these effects are most likely several orders of
301 magnitude smaller compared to the large range in dissolved Mn in pore water. Since
302 pore water Mn is the dominant factor controlling Mn incorporation, studies must
303 account for ecological controls, like foraminiferal depth habitat preference, as well as

304 for geochemical controls like oxygen concentrations and organic matter fluxes (Koho
305 et al., 2015; De Lange, 1986; Reichart et al., 2003). The fact that this study was based
306 on living foraminifera circumvents potential complications due to Mn-rich coatings.
307 Such coatings would likely not affect the aragonitic shell of *H. elegans* (Ní Fhlaithearta
308 et al., 2010), but might interfere when analyzing fossil calcite shells. Still, a spatially
309 resolved analytical technique like LA-ICP-MS allows detecting such coatings also in
310 fossil specimens.

311

312 **4.1 Impact of redox conditions and foraminiferal habitat preference** 313 **on Mn incorporation**

314 In general, flux of organic matter arriving at the sea floor decreases with increasing
315 water depth, due to ongoing degradation during settling (Arndt et al., 2013 and
316 references therein). Consequently, redox boundaries within the sediment generally also
317 deepen as a function of water depth, as oxygen consumption in the sediment decreases.
318 Such a fundamental organic matter-depth relation is in line with the much deeper
319 oxygen penetration depths at stations A and B compared to the more shallow stations.
320 At station F the relative shallow oxygen penetration depth observed is in line with its'
321 relative shallow water depth, although the organic matter which arrives here at the
322 seafloor apparently undergoes winnowing (Fontanier et al., 2008). The organic matter
323 along the transect studied is concentrated at a so-called depocenter, which largely
324 coincides with the depths of stations C and D (Fontanier et al., 2008). As bottom waters
325 at all stations are well oxygenated, organic matter concentration can be considered the
326 main control for redox conditions at stations F-A, with the amount of organic matter
327 arriving at the seabed being regulated by water depth and sedimentary processes, such
328 as focusing versus winnowing.

329 At stations C, D and F, the oxygen penetration depth and the Mn²⁺ redox
330 boundaries are at the same depth, as expected. Station F shows the shallowest OPD of
331 all stations, although the organic matter concentration is relatively low. One explanation
332 for this observation is that a lower porosity at F (56% versus 76% and 79 % at stations
333 D and E, respectively) impedes oxygen diffusion through the sediment. Alternatively,
334 the pore water profile reflects an earlier organic matter deposition event, with this
335 organic matter being largely consumed at the time of sampling. The pore water profiles
336 require more time to re-equilibrate to the new conditions (Burdige and Gieskes, 1983).
337 At station E there is a mismatch between oxygen penetration depth and the Mn²⁺ redox
338 boundary as the Mn²⁺ redox boundary is considerably deeper than the OPD. Although
339 this is in line with the observed higher bioirrigation at this station (Fontanier et al.,
340 2008), this might reflect non-equilibrium conditions as well.

341 The vertical distribution of benthic foraminiferal species varies between
342 stations, in accordance with organic matter concentrations and redox zonation, which
343 is consistent with the TROX model (Jorissen et al., 1995; Fontanier et al., 2008). In
344 case of a shallower redox zone, infaunal benthic foraminifera biomineralize in contact
345 with Mn-enriched pore water, with highest dissolved manganese concentrations
346 occurring just below the oxygen penetration depth at all stations, except for station E
347 (552 m). This is in contrast to low bottom-water oxygen environments often studied in
348 the context of proxy development studies, where pore water Mn²⁺ is released from the
349 pore water (Koho et al., 2015, 2017; Mangini et al., 2001).

350 The species studied here cover the range of shallow-infauna to intermediate-
351 infauna niches. Both *Uvigerina mediterranea* and *M. barleeanus* were in the Gulf of
352 Lyons found to occupy shallow to intermediate infaunal habitat, with *U. peregrina*
353 having a somewhat shallower infaunal habitat (Fontanier et al., 2008). *Hoeglundina*

354 *elegans*, a typically shallow infaunal species, is often found close to the sediment-water
355 interface (Jorissen et al., 1998; Schönfeld 2001; Fontanier et al., 2002; Fontanier et al.,
356 2008) and contains the lowest concentration of Mn in its test. Only at the shallowest
357 station (350 m) three specimens of *H. elegans* show concentrations above the detection
358 level, with values still low compared to the values observed for the other species (Fig.
359 6). In the Bay of Biscay Reichart et al. (2003) also suggested that elevated Mn
360 concentrations in *H. elegans* were confined to stations with oxygen depleted bottom
361 waters and/or with a shallow oxygen penetration depth. *Uvigerina mediterranea* and
362 *Uvigerina peregrina* are also classed as shallow-infaunal species; they are typically
363 found within the top few centimeters of the sediment column (Fontanier et al. 2002,
364 Fontanier et al. 2008). The calculated average living depth (ALD₁₀) as calculated in
365 Fontanier et al. (2008) is consistently shallower than the ALD₁₀ for *U. mediterranea*.
366 This is at odds with previous reports suggesting *U. peregrina* has a slightly deeper
367 microhabitat than *U. mediterranea* (Fontanier et al. 2002; 2006). That *U. peregrina* has
368 a deeper microhabitat is further supported by the usual distinct $\delta^{13}\text{C}$ offset in *U.*
369 *peregrina*, which is more depleted compared to *U. mediterranea* (Schmiedl et al., 2004;
370 Fontanier et al, 2002, 2006). The higher Mn/Ca values observed here for *U. peregrina*
371 (Figure 6) supports the idea that it calcifies somewhat deeper in the sediment compared
372 to *U. mediterranea*. Alternatively, *U. peregrina* may migrate downwards within
373 burrows to track food resources, recording redox steepness (Loubere et al., 1995). This
374 could highlight a disparity between the assumed living depth (the depth interval of
375 recovery) and biomineralization depth of foraminifera. Still, this would also result in a
376 higher variability of Mn/Ca values at higher Mn/Ca levels, which is not observed.
377 Hence, more likely the observed disparity between the geochemical signals
378 incorporated into foraminiferal calcite and depth of recovery in *U. peregrina* reflects

379 opportunistic behaviour, with calcification at a shallower in-sediment depth in response
380 to more favourable conditions after e.g. seasonal peaks in organic matter fluxes
381 (Accornero et al., 2003), when the OPD is close to the sediment water interface.

382 *Melonis barleeanus*, generally considered an intermediate-infaunal species
383 (Fontanier et al., 2002, 2008), contains the highest concentrations of Mn in its test,
384 which is in line with the deepest habitat of the species studied here. Manganese
385 incorporation in this species increases with increasing labile organic matter (Fig. 7a).

386 In summary, the habitat preference of the benthic foraminiferal species studied
387 here is reflected in the Mn/Ca values recorded in their tests. This is in contrast with
388 other results showing lower Mn/Ca values in foraminiferal tests with shallower redox
389 fronts (Koho et al., 2015). This, however, critically depends on the Mn being released
390 to the water column, which only occurs when the bottom waters are disoxic. In case of
391 a seasonal organic matter deposition event, an increase of Mn concentration in
392 foraminiferal test carbonate would initially occur in the deeper and ultimately also in
393 the more shallow calcifying foraminifera. This is in line with the conceptual
394 TROXCHEM³ model, with the conditions studied here falling within the first stage of
395 the temporal succession considered in the model. Bottom water remains well
396 oxygenated (O₂ concentrations at the study area: 199-219 μmol/l (Fontanier et al.,
397 2008)) and organic matter loading is controlling Mn²⁺ concentrations in the sediment.
398 To what extent species are high in Mn/Ca depends on living depth and opportunistic
399 behavior.

400 At a given location, a benthic foraminiferal species' depth preference or
401 biomineralization depth, is reflected in its average Mn/Ca value (Fig. 5). The trend
402 across a depth transect shows a strong correlation to labile organic matter
403 concentrations in the surface sediments (Fig. 7). The strong correlation between labile

404 organic matter (i.e. sedimentary lipid content) and Mn incorporation in shallow and
405 intermediate infaunal species *U. mediterranea* ($R^2 = 0.80$ ($p < 0.05$)) suggests that test
406 Mn has potential as a proxy for detecting past labile organic matter fluxes. Notably,
407 *M. barleeanus* has a very strong correlation (0.81), though this correlation lacks
408 statistical significance ($p > 0.05$). In contrast, *U. peregrina* shows a correlation
409 coefficient of only 0.45 (R^2) between test Mn and labile organic matter. *Uvigerina*
410 *peregrina* is reported to respond opportunistically to the concentration and quality of
411 organic matter produced during bloom events (Fontanier et al., 2003; Koho et al., 2008;
412 Barras et al., 2010). This response is in the form of increased reproduction and growth.
413 Perhaps *U. peregrina* calcifies preferentially at shallower depths and therefore does not
414 capture the full Mn^{2+} gradient.

415 At low oxygen concentrations Mn is released through the reduction of
416 manganese (oxy)hydroxides. Here we show an increase in Mn/Ca incorporation in
417 several species, from shallow to intermediate-depth infaunal habitats, as a function of
418 oxygen penetration depth. Such a correlation agrees with studies by Ní Fhlaithearta et
419 al. (2010) and McKay et al. (2015) from a down core record of $Mn/Ca_{H.elegans}$ during the
420 formation of sapropel (S1) in the Eastern Mediterranean and a paleoproductivity study
421 of an upwelling system in the NE Atlantic, respectively. Here, a comparison of Mn
422 (oxy)hydroxides in the sediment and foraminiferal Mn^{2+} showed that Mn^{2+}
423 incorporation in an epifaunal to shallow infaunal species was higher during times of
424 enhanced Mn^{2+} remobilization and hence higher pore water Mn^{2+} . Such a correlation,
425 however, requires that the bottom waters remain somewhat oxygenated to retain the
426 dissolved Mn^{2+} in the pore water. With disoxic bottom waters Mn^{2+} escapes the
427 porewater and foraminiferal Mn/Ca values decrease (Koho et al., 2015). However, with
428 high organic matter deposition, which might be concentrated in events, also

429 foraminiferal species living at or close to the sediment water interface may show
430 elevated Mn concentrations.

431 In addition to the here observed changes, biomineralization could affect Mn^{2+}
432 incorporation. In a controlled laboratory study by Munsel et al (2010) Mn
433 incorporation in *Ammonia tepida* increased with increasing Mn^{2+} concentrations in the
434 culture water and the partition coefficient was well above 1. The lack of an
435 appreciable discrimination argues against a major biomineralization impact on Mn^{2+}
436 partitioning. Recently Barras et al. (2018), also using controlled growth experiments,
437 showed, however, that Mn partitioning in *B. marginata* differs from that in *A. tepida*,
438 with that in *B. marginata* being close to one and that of *A. tepida* being 4 times lower.
439 Inter-specific differences are considerable and hence an impact of biomineralization
440 on Mn incorporation can not be disregarded .

441 In summary, Mn incorporation seems primarily controlled by pore water
442 conditions in close proximity to the test, biomineralization and with a secondary
443 control determined by the ability of a foraminifer to seasonally calcify and migrate
444 within the sediment.

445 446 **4.2 Pore water Mn dynamics and foraminiferal migration within the sediment**

447 Manganese is incorporated in foraminiferal carbonate with a partition coefficient (D)
448 close to 1 or somewhat lower (Munsel et al., 2010; Barras et al., 2018). We calculated
449 Mn partition coefficients for *U. mediterranea*, *U. peregrina* and *M. barleeanus* at
450 stations E, C and B (Table 6) based on average Mn/Ca_{foram} and average $Mn/Ca_{\text{pore water}}$
451 values found above the Mn^{2+} - $MnO(H)$ redox boundary. Calculated D_{Mn} agrees with the
452 previously reported D_{Mn} by Munsel et al., (2010), with values varying between ~1-2 for
453 *U. mediterranea* and *U. peregrina*. The Mn partition coefficient for *Melonis barleeanus*
454 ranges from ~4-7. The partition coefficient for this species most likely reflects its

455 capacity to calcify under dysoxic conditions, close to or even below the oxygen
456 penetration depth. Still, this calculation is based on two assumptions: (1) the depth
457 foraminifera are recovered from during sampling corresponds with the average depth
458 of calcification and, (2) variation in pore water is limited. Establishing species specific
459 Mn partitioning coefficients using culture experiments might, however, be needed for
460 unlocking the full potential of this proxy (Barras et al., 2018).

461 A foraminifer calcifying within a steep Mn^{2+} gradient is exposed to a higher
462 range of Mn^{2+} concentrations (over a fixed depth interval) compared to specimens living
463 along a more gradual Mn^{2+} concentration gradient. Since foraminifera can migrate
464 through the sediment as a response to food availability and oxygen concentrations (Alve
465 and Bernhard 1995; Gross, 2000), not only the slope of the Mn gradient, but also the
466 in-sediment depth range (microhabitat) of the foraminifer in relation to the Mn redox
467 boundary, should be considered (Fig. 8). Although the analyses of foraminiferal test
468 Mn/Ca is challenging, which adds to the inter-specimen variability, we observe
469 systematic differences between species in Mn/Ca variability. A shallow-infauna
470 species, with a limited in-sediment range, would be expected to exhibit lower variability
471 than an intermediate- infauna species, which possibly migrates considerably in depth.
472 This is exemplified at station F (350 m) where we note an increase in foraminiferal test
473 Mn/Ca variability at 2 cm depth, consistent with the oxygen penetration depth at that
474 station (Fig. 3). Moreover, the variability in Mn/Ca values increases towards higher
475 Mn/Ca values. This is in line with the depth habitat of *M. barleeanus* being consistently
476 deeper and this species traveling more actively through the redox zones than *U.*
477 *mediterranea* or *U. peregrina*. Nitrate respiration could be mechanism allowing this
478 dynamic behaviour by *M. barleeanus* in the intermediate depth habitat. However, Pina-
479 Ochoa et al. (2010), studying denitrification in foraminifera, reports nitrate storage in

480 all three species mentioned here. Notably, nitrate storage in *M. barleeanus* is lower than
481 *U. mediterranea* and *U. peregrina*. Alternatively *M. barleeanus* thrives in habitats with
482 varying oxygenation and hence also varying Mn levels, whereas the stable but high
483 Mn/Ca values in the Uvigerinids are related to their opportunistic behaviour.

484 With a redox-sensitive element such as Mn, in a dynamic geochemical
485 environment, it is not surprising that foraminifera exhibit high inter-individual
486 variability in their Mn/Ca incorporation. Benthic foraminifera reside in a 3D
487 geochemical mosaic, as reflected by a large spread of Mn values, in addition to
488 undergoing substantial temporal variability. Still, using Mn/Ca as a potential proxy for
489 redox conditions or primary productivity seems promising, as established ecological
490 characteristics of species are reflected by differences in Mn incorporation. Apparently
491 the large variability on both spatial and temporal scales averages out, making Mn into
492 a promising proxy for paleo-redox and organic matter flux.

493

494 **5. Conclusion**

495 This study investigates the link between benthic foraminiferal habitat preferences and
496 manganese incorporation in their tests. Manganese incorporation increases with
497 bottom-arriving labile organic matter content, driven by enhanced oxygen demand.
498 This results in a more shallow oxygen penetration depth with immediately below it
499 enhanced dissolved Mn levels. Shallow infaunal species calcify under lower
500 concentrations of Mn compared to intermediate infauna, in line with their depth
501 preference. Their depth habitat is related to in-sediment changes in redox conditions.
502 However, these distribution not necessarily vary synchronous with changes in redox
503 zonation as illustrated by the Mn/Ca variability in their tests (Fig. 8). The latter reflects
504 the Mn/Ca porewater composition, which itself is directly related to reactive organic

505 matter concentration and redox conditions. The foraminiferal Mn/Ca ratio and inter-
506 specimen variability, therefore, provides information on past Mn cycling within the
507 sediment. Consequently, foraminiferal Mn/Ca ratio is a potential proxy for bottom-
508 water oxygenation and organic matter fluxes.

509

510 **Acknowledgements**

511 We thank captain and crew of the N/O *Téthys 2* (CNRS-INSU) for their assistance
512 during the *BEHEMOTH* campaign. We acknowledge the technical assistance given by
513 Christine Barras, Mélissa Gaultier, Sophie Terrien and Gérard Chabaud from Angers
514 and Bordeaux University. We thank Serge Berné and Laetitia Maltese (Ifremer), for
515 providing us with maps of the study area and Xavier Durrieu de Madron (Perpignan
516 University) for discussions about water column structure. Helen de Waard (LA-ICP-
517 MS) and Karoliina Koho (SEM) (Utrecht University) are acknowledged for their
518 laboratory assistance. The associate editor and two anonymous reviewers are
519 acknowledged for their helpful comments. The Darwin Center for Biogeosciences
520 provided partial funding for this project. This paper contributes to the Netherlands Earth
521 Systems Science Center (NESSC –www.nessc.nl)

522

523 **References**

- 524 Accornero, A., Picon, P., De Bovée, F., Charrière, B., & Buscail, R.: Organic carbon
525 budget at the sediment–water interface on the Gulf of Lions continental margin.
526 *Continental Shelf Research*, 23(1), 79-92, 2003.
- 527
528 Alve, E., & Bernhard, J. M.: Vertical migratory response of benthic foraminifera to
529 controlled oxygen concentrations in an experimental mesocosm. *Oceanographic*
530 *Literature Review*, 9(42), 771, 1995.
- 531
532
533 Arndt, S., Jørgensen, B. B., LaRowe, D. E., Middelburg, J. J., Pancost, R. D. and
534 Regnier, P.: Quantifying the degradation of organic matter in marine sediments: A
535 review and synthesis, *Earth-Science Rev.*, 123, 53–86,

536 doi:10.1016/j.earscirev.2013.02.008, 2013.
537
538 Barnett, P. R. O., Watson, J. and Connely, D.: A multiple corer for taking virtually
539 undisturbed sample from shelf, bathyal and abyssal sediments, *Oceanologica Acta*, 7,
540 399-408, 1984.
541
542 Barras, C., Fontanier, C., Jorissen, F. and Hohenegger, J.: A comparison of spatial and
543 temporal variability of living benthic foraminiferal faunas at 550 m depth in the Bay
544 of Biscay, *Micropaleontology*, 56, 275-295, 2010.
545
546 Barras, C., Mouret, A., Nardelli, M.P., Metzger, E., Petersen, J., La, C., Filipsson,
547 H.L., Jorissen, F.: Experimental calibration of manganese incorporation in
548 foraminiferal calcite, *Geochim. Cosmochim. Acta*, 237, 49-64, 2018.
549
550 Boyle, E. A.: Manganese carbonate overgrowths on foraminifera tests, *Geochim.*
551 *Cosmochim. Acta*, 47, 1815-1819, DOI: 10.1016/0016-7037(83)90029-7, 1983.
552
553 Burdige, D. J. and Gieskes, J. M. : A pore water/solid phase diagenetic model for
554 manganese in marine sediments. *American Journal of Science*, 283(1), 29-47, 1983.
555
556 De Lange, G. J.: Early diagenetic reactions in interbedded pelagic and turbiditic
557 sediments in the Nares Abyssal Plain (western North Atlantic): Consequences for the
558 composition of sediment and interstitial water, *Geochim. Cosmochim. Acta*, 50(12),
559 2543–2561, doi:10.1016/0016-7037(86)90209-7, 1986.
560
561 Dueñas-Bohórquez, A., Rocha, R., Kuroyanagi, A., de Nooijer, L., Bijma, J.,
562 Reichart, G.J.: Interindividual variability and ontogenetic effects on Mg and Sr
563 incorporation in the planktonic foraminifer *Globigerinoides sacculifer*. *Geochim.*
564 *Cosmochim. Acta*, 75 (2), 520-532, 2011.
565
566 Elderfield, H., Yu, J., Anand, P., Kiefer, T. and Nyland, B.: Calibrations for benthic
567 foraminiferal Mg/Ca paleothermometry and the carbonate ion hypothesis, *Earth*
568 *Planet. Sci. Lett.*, 250(3–4), 633–649, doi:10.1016/j.epsl.2006.07.041, 2006.
569
570 Fontanier, C., Jorissen, F. J., Licari, L., Alexandre, A., Anschutz, P. and Carbonel, P.:
571 Live benthic foraminiferal faunas from the Bay of Biscay: faunal density,
572 composition, and microhabitats, *Deep Sea Research Part I: Oceanographic Research*
573 *Papers*, 49, 751-785, DOI: 10.1016/S0967-0637(01)00078-4, 2002.
574
575 Fontanier, C., Jorissen, F. J., David, C., Anschutz, P., Chaillou, G. and Lafon, V.:
576 Seasonal and interannual variability of benthic foraminiferal faunas at 550m depth in
577 the Bay of Biscay. *Deep-Sea Research I*, 50, 457-494, 2003.
578
579 Fontanier, C., Mackensen, A., Jorissen, F. J., Anschutz, P., Licari, L., & Griveaud, C.:
580 Stable oxygen and carbon isotopes of live benthic foraminifera from the Bay of
581 Biscay: Microhabitat impact and seasonal variability. *Marine Micropaleontology*,
582 58(3), 159-183, 2006.
583
584 Fontanier, C., Jorissen, F. J., Lansard, B., Mouret, A., Buscail, R., Schmidt, S.,
585 Kerhervé, P., Buron, F., Zaragosi, S., Hunault, G., Ernoult, E., Artero, C., Anschutz,

586 P. and Rabouille, C.: Live foraminifera from the open slope between Grand Rhône
587 and Petit Rhône Canyons (Gulf of Lions, NW Mediterranean), *Deep. Res. Part I*
588 *Oceanogr. Res. Pap.*, 55(11), 1532–1553, doi:10.1016/j.dsr.2008.07.003, 2008.
589

590 Froelich P. N., Klinkhammer G. P., Bender M. L., Luedtke N. A., Heath G. R., Cullen
591 D., Dauphin P., Hammond D., Hartman B. and Maynard V.: Early oxidation of
592 organic matter in pelagic sediments of the eastern equatorial Atlantic: suboxic
593 diagenesis. *Geochim. Cosmochim. Acta* 43(1075), 1090, 1979.

594 Glock, N., Eisenhauer, A., Liebetrau, V., Wiedenbeck, M., Hensen, C. and Nehrke,
595 G.: EMP and SIMS studies on Mn/Ca and Fe/Ca systematics in benthic foraminifera
596 from the Peruvian OMZ: A contribution to the identification of potential redox
597 proxies and the impact of cleaning protocols, *Biogeosciences*, 9(1), 341–359,
598 doi:10.5194/bg-9-341-2012, 2012.
599

600 Groeneveld, J. and Filipsson, H. L.: Mg/Ca and Mn/Ca ratios in benthic foraminifera:
601 the potential to reconstruct past variations in temperature and hypoxia in shelf
602 regions, *Biogeosciences*, 10(7), 5125–5138, doi:10.5194/bg-10-5125-2013, 2013.
603

604 Gross, O.: Influence of temperature, oxygen and food availability on the migrational
605 activity of bathyal benthic foraminifera: evidence by microcosm experiments. In *Life*
606 *at Interfaces and Under Extreme Conditions* (pp. 123-137). Springer Netherlands,
607 2000.
608

609 Hintz, C. J., Shaw, T. J., Chandler, G. T., Bernhard, J. M., McCorkle, D. C. and
610 Blanks, J. K.: Trace/minor element δ : calcium ratios in cultured benthic foraminifera.
611 Part I: Inter-species and inter-individual variability, *Geochim. Cosmochim. Acta*,
612 70(8), 1952–1963, doi:10.1016/j.gca.2005.12.018, 2006a.
613

614 Jochum, K. P., Weis, U., Stoll, B., Kuzmin, D., Yang, Q., Raczek, I., Jacob, D. E.,
615 Stracke, A., Birbaum, K., Frick, D. A., Gunther, D., Enzweiler, J.:
616 Determination of Reference Values for NIST SRM 610-617 Glasses Following ISO
617 Guidelines, *Geostandards and Geoanalytical Research*, 35, 4, 397-421, 2011.
618

619 Jorissen, F. J., de Stigter, H. C. and Widmark, J. G. V: A conceptual model explaining
620 benthic foraminiferal microhabitats, *Mar. Micropaleontol.*, 26(1–4), 3–15,
621 doi:10.1016/0377-8398(95)00047-X, 1995.
622

623 Jorissen, F. J., Wittling, I., Peypouquet, J. P., Rabouille, C. and Relexans, J. C.: Live
624 benthic foraminiferal faunas off Cape Blanc, NW-Africa: Community structure and
625 microhabitats, *Deep Sea Research Part I: Oceanographic Research Papers*, 45, 2157-
626 2188, DOI: 10.1016/S0967-0637(98)00056-9, 1998.
627

628 Koho, K. A., Langezaal, A. M., van Lith, Y. A., Duijnste, I. A. P. and van der
629 Zwaan, G. J.: The influence of a simulated diatom bloom on deep-sea benthic
630 foraminifera and the activity of bacteria: A mesocosm study, *Deep. Res. Part I*
631 *Oceanogr. Res. Pap.*, 55(5), 696–719, doi:10.1016/j.dsr.2008.02.003, 2008.
632

633 Koho, K. A., Piña-Ochoa, E., Geslin, E. and Risgaard-Petersen, N.: Vertical
634 migration, nitrate uptake and denitrification: Survival mechanisms of foraminifera

635 (Globobulimina turgida) under low oxygen conditions, FEMS Microbiol. Ecol., 75(2),
636 273–283, doi:10.1111/j.1574-6941.2010.01010.x, 2011.

637

638 Koho, K. A., de Nooijer, L. J. and Reichart, G. J.: Combining benthic foraminiferal
639 ecology and shell Mn/Ca to deconvolve past bottom water oxygenation and
640 paleoproductivity, Geochim. Cosmochim. Acta, 165, 294–306,
641 doi:10.1016/j.gca.2015.06.003, 2015.

642

643 Koho, K. A., De Nooijer, L. J., Fontanier, C., Toyofuku, T., Oguri, K., Kitazato, H.
644 and Reichart, G. J.: Benthic foraminiferal Mn / Ca ratios reflect microhabitat
645 preferences, Biogeosciences, 14(12), 3067–3082, doi:10.5194/bg-14-3067-2017, 2017

646

647 Lea, D. and Boyle, E.: Barium content of benthic foraminifera controlled by bottom-
648 water composition, Nature, 338, 751-753, 1989.

649

650 Lewis, E., and Wallace, D. W. R.: Program Developed for CO2 Systems Calculations.
651 ORNL/CDIAC-105, Carbon Dioxide Information Analysis Centre, Oak Ridge
652 National Laboratory U.S. Department of Energy, Oak Ridge, Tennessee, 1998.

653

654 Loubere, P., Meyers, P., and Gary, A.: Benthic foraminiferal microhabitat selection,
655 carbon isotope values, and association with larger animals: A test with uvigerina
656 peregrina, Journal of Foraminiferal Research, 25, 83-95. DOI:10.2113/gsjfr.25.1.83,
657 1995.

658

659 Mangini, A., Jung, M. and Laukenmann, S.: What do we learn from peaks of uranium
660 and of manganese in deep sea sediments?, Mar. Geol., 177(1–2), 63,
661 doi:10.1016/S0025-3227(01)00124-4, 2001.

662

663 McKay, C. L., Groeneveld, J., Filipsson, H. L., Gallego-Torres, D., Whitehouse, M.
664 J., Toyofuku, T. and Romero, O. E.: A comparison of benthic foraminiferal Mn / Ca
665 and sedimentary Mn / Al as proxies of relative bottom-water oxygenation in the low-
666 latitude NE Atlantic upwelling system, Biogeosciences, 12(18), 5415–5428,
667 doi:10.5194/bg-12-5415-2015, 2015.

668

669 Munsel, D., Kramar, U., Dissard, D., Nehrke, G., Berner, Z., Bijma, J., Reichart, G. J.
670 and Neumann, T.: Heavy metal incorporation in foraminiferal calcite: Results from
671 multi-element enrichment culture experiments with Ammonia tepida, Biogeosciences,
672 7(8), 2339–2350, doi:10.5194/bg-7-2339-2010, 2010.

673

674 Ní Fhlaithearta, S., Reichart, G.-J., Jorissen, F.J., Fontanier, C., Rohling, E.J.,
675 Thomson, J. & de Lange, G.J.: Reconstructing the seafloor environment during
676 sapropel formation using benthic foraminiferal trace metals, stable isotopes, and
677 sediment composition. *Paleoceanography*, 25(4), 2010. DOI:10.1029/2009PA001869

678

679 Ní Fhlaithearta, S., Ernst, S. R., Nierop, K. G. J., de Lange, G. J. and Reichart, G.-J.:
680 Molecular and isotopic composition of foraminiferal organic linings, Mar.
681 Micropaleontol., 102, doi:10.1016/j.marmicro.2013.06.004, 2013.

682

683 Nürnberg, D., Bijma, J. and Hemleben, C.: Assessing the reliability of magnesium in
684 foraminiferal calcite as a proxy for water mass temperatures, *Geochim. Cosmochim.*
685 *Acta*, 60(5), 803–814, doi:10.1016/0016-7037(95)00446-7, 1996.
686

687 Pina-Ochoa, E., Hogslund, S., Geslin, E., Cedhagen, T., Revsbech, N. P., Nielsen, L.
688 P., Schweizer, M., Jorissen, F., Rysgaard, S. and Risgaard-Petersen, N.: Widespread
689 occurrence of nitrate storage and denitrification among Foraminifera and Gromiida,
690 *Proc. Natl. Acad. Sci.*, 107(3), 1148–1153, doi:10.1073/pnas.0908440107, 2010.
691

692 Reichart, G. J., Jorissen, F., Anschutz, P. and Mason, P. R. D.: Single foraminiferal
693 test chemistry records the marine environment, *Geology*, 31(4), 355–358,
694 doi:10.1130/0091-7613(2003)031<0355:SFTCRT>2.0.CO;2, 2003.
695

696 Risgaard-Petersen, N., Langezaal, A. M., Ingvarsdén, S., Schmid, M. C., Jetten, M. S.
697 M., Op Den Camp, H. J. M., Derksen, J. W. M., Piña-Ochoa, E., Eriksson, S. P.,
698 Nielsen, L. P., Revsbech, N. P., Cedhagen, T. and Van Der Zwaan, G. J.: Evidence for
699 complete denitrification in a benthic foraminifer, *Nature*, 443(7107), 93–96,
700 doi:10.1038/nature05070, 2006.
701

702 Rosenthal, Y., Morley, A., Barras, C., Katz, M. E., Jorissen, F., Reichart, G.-J., Oppo,
703 D. W. and Linsley, Braddock. K.: Temperature calibration of Mg/Ca ratios in the
704 intermediate water benthic foraminifera *Hyalinea Balthica*, *Geochem. Geophys.*
705 *Geosyst.*, 12(4), 2011. doi: 10.1029/2010GC003333
706

707 Schönfeld, J.: Benthic foraminifera and pore water oxygen profiles: A reassessment of
708 species boundary conditions at the Western Iberian margin, *Journal of Foraminiferal*
709 *Research*, 31, 86-107, 10.2113/0310086, 2001.
710

711 Schmiidl, G., Pfeilsticker, M., Hemleben, C., Mackensen, A.: Environmental and
712 biological effects on the stable isotope composition of recent deep-sea benthic
713 foraminifera from the western Mediterranean Sea *Mar. Micropaleontol.*, 51, 129–152
714 <http://dx.doi.org/10.1016/j.marmicro.2003.10.001>, 2004.
715

716 Van Cappellen, P. and Wang, Y.: Cycling of iron and manganese in surface
717 sediments: A general theory for the coupled transport and reaction of carbon, oxygen,
718 nitrogen, sulfur, iron, and manganese, *Am. J. Sci.*, 296(3), 197–243,
719 doi:10.2475/ajs.296.3.197, 1996.
720

721 Wang, Y. and Van Cappellen, P.: A multicomponent reactive transport model of early
722 diagenesis: Application to redox cycling in coastal marine sediments, *Geochim.*
723 *Cosmochim. Acta*, 60(16), 2993–3014, doi:10.1016/0016-7037(96)00140-8, 1996.
724

725 Wit, J. C., De Nooijer, L. J., Barras, C., Jorissen, F. J. and Reichart, G. J.: A
726 reappraisal of the vital effect in cultured benthic foraminifer *Bulimina marginata* on
727 Mg/Ca values: Assessing temperature uncertainty relationships, *Biogeosciences*, 9(9),
728 3693–3704, doi:10.5194/bg-9-3693-2012, 2012.
729

730 Yu, J. and Elderfield, H.: Benthic foraminiferal B/Ca ratios reflect deep water
731 carbonate saturation state, *Earth Planet. Sci. Lett.*, 258(1–2), 73–86,
732 doi:10.1016/j.epsl.2007.03.025, 2007.

733
734
735

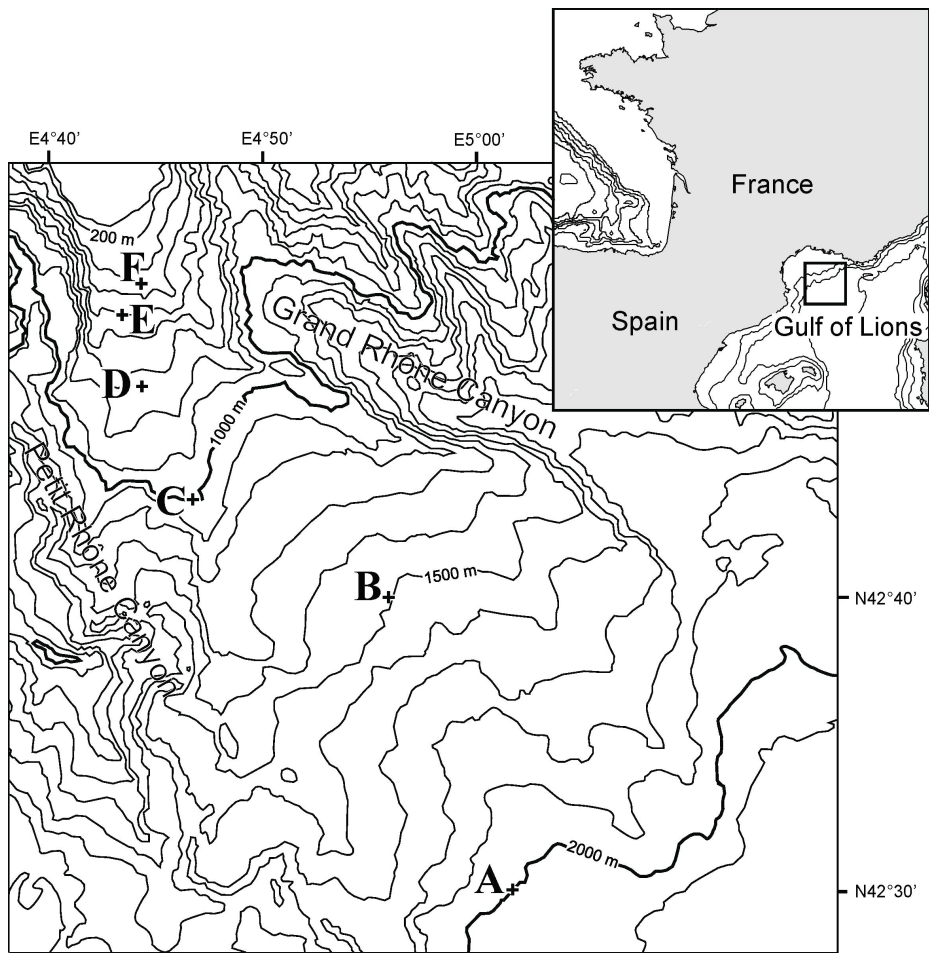


Figure 1. Location map showing sampling stations and bathymetry.

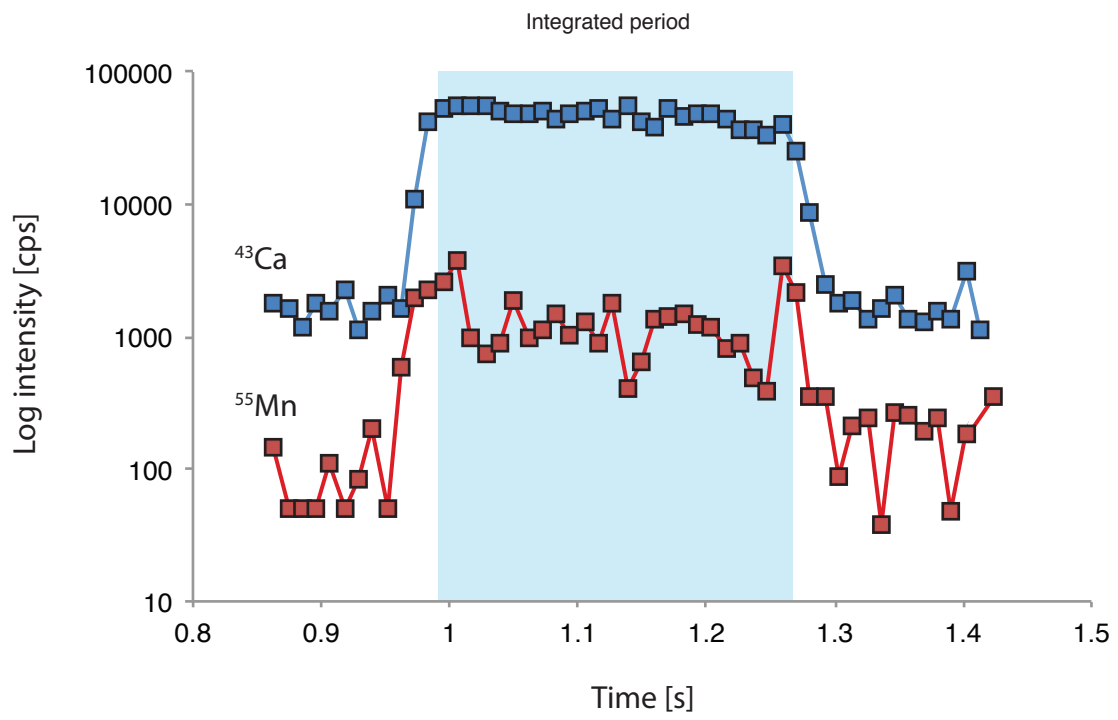


Figure 2. Example of a laser ablation profile, signal log intensity counts per second [cps] through time. The integrated signal is shaded.

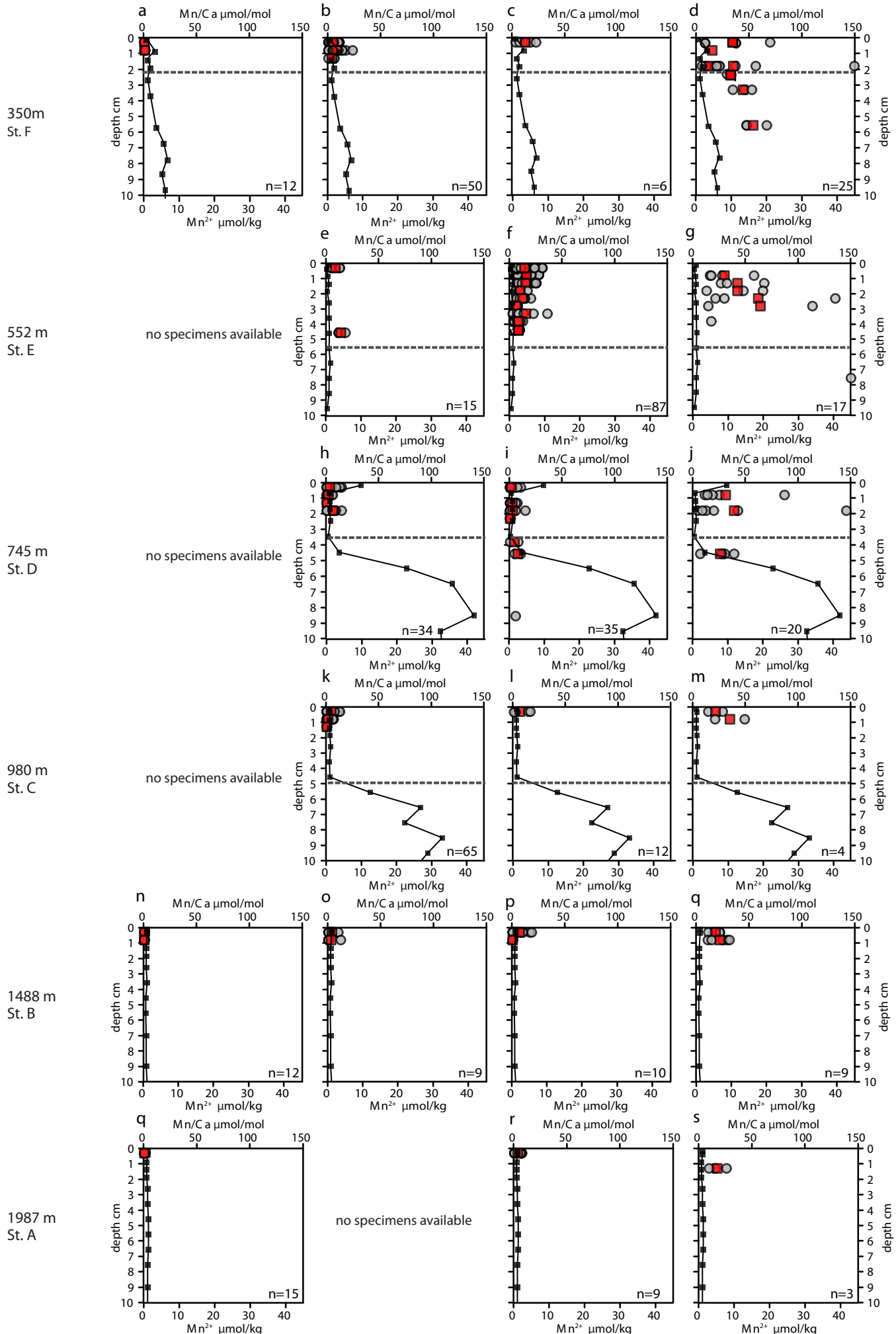
*H. elegans**U. mediterranea**U. peregrina**M. barleeanus*

Figure 3. Plots of Mn/Ca ($\mu\text{mol/mol}$) measured in living (stained) *Hoeglundina elegans*, *Uvigerina mediterranea*, *Uvigerina peregrina* and *Melonis barleeanus*. Individual analyses are plotted (grey circles) alongside average values for a given depth in the sediment (red squares). Porewater Mn²⁺ ($\mu\text{mol/kg}$) profiles (black line) are plotted for all stations. The dashed grey line indicates the oxygen penetration depth (OPD).

Figure 4.

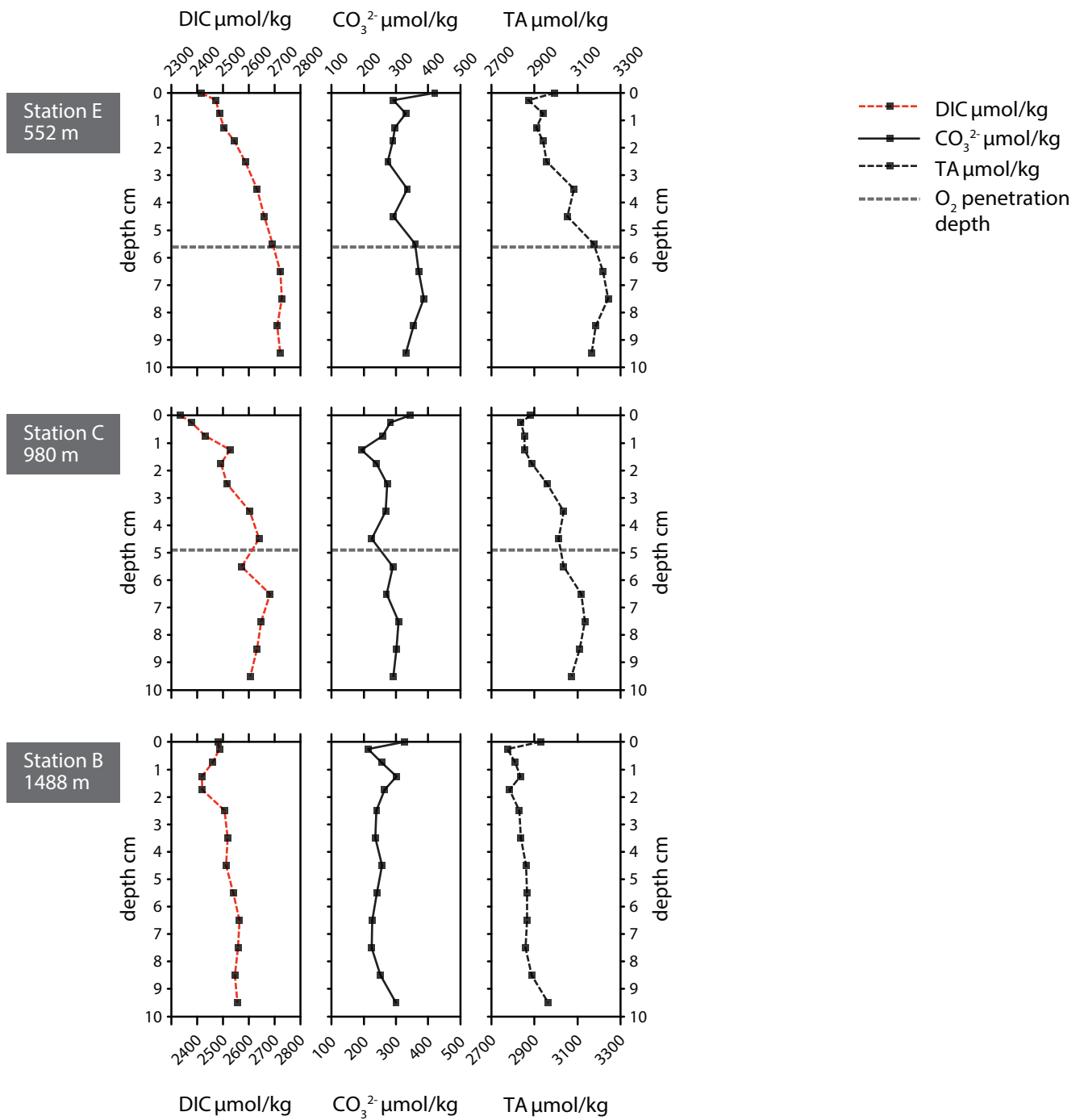


Figure 4. Carbonate chemistry parameters for stations E, C and B. A) Dissolved inorganic carbon (DIC), B) $[\text{CO}_3^{2-}]$ in $\mu\text{mol/kg}$, C) Total alkalinity (TA) in $\mu\text{mol/kg}$.

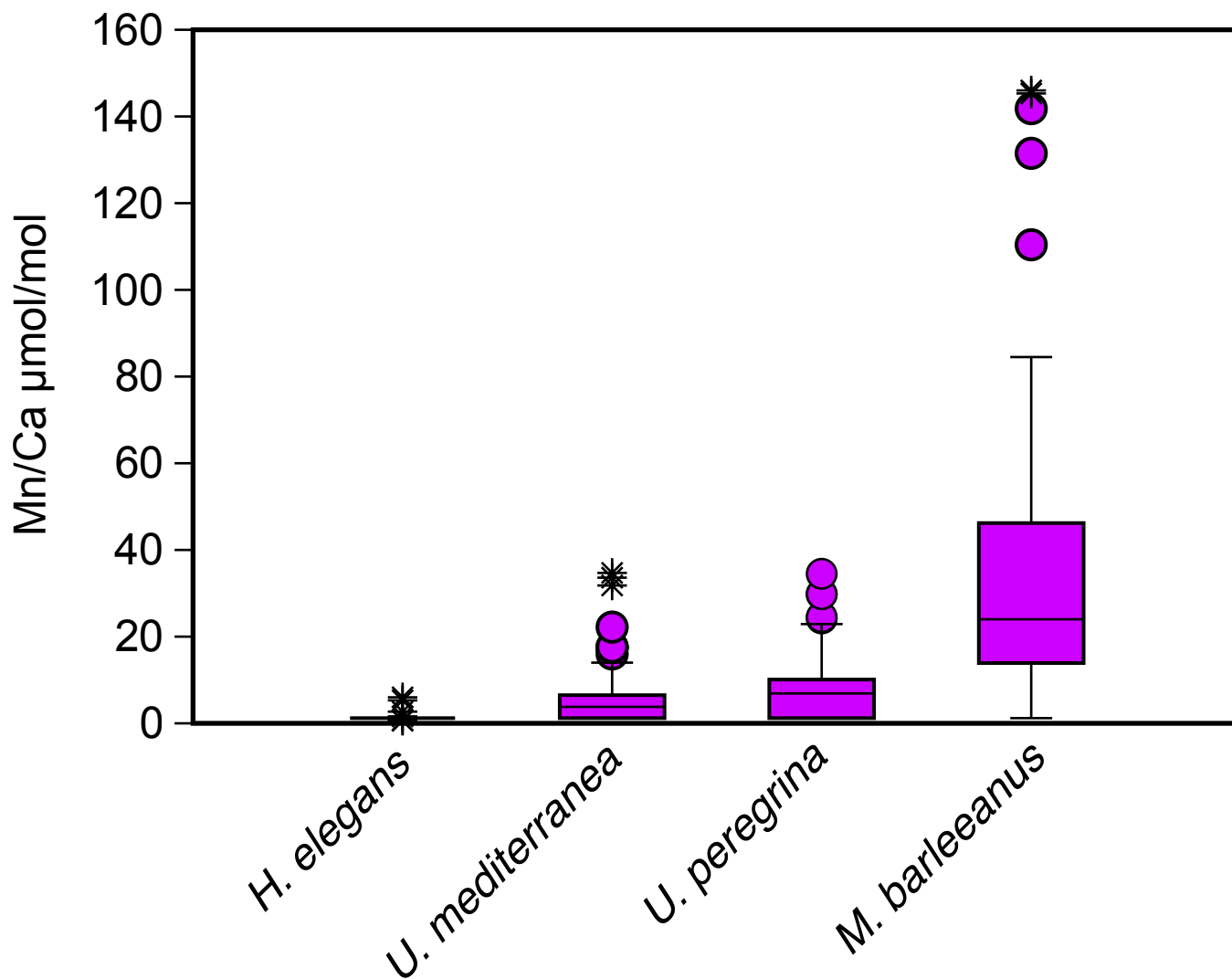


Figure 5. Box plots describing the distribution in Mn/Ca values measured in living (stained) individuals of *Hoeglundina elegans*, *Uvigerina mediterranea*, *Uvigerina peregrina* and *Melonis barleeanus*. The box represents all values between the 25th and 75th percentile. The dissection line through the box denotes the median. The whiskers are drawn from the top of the box up to the largest data point less than 1.5 times the box height from the box and similarly below the box. Values outside the whiskers are shown as circles, values further than 3 times the box height are denoted as stars.

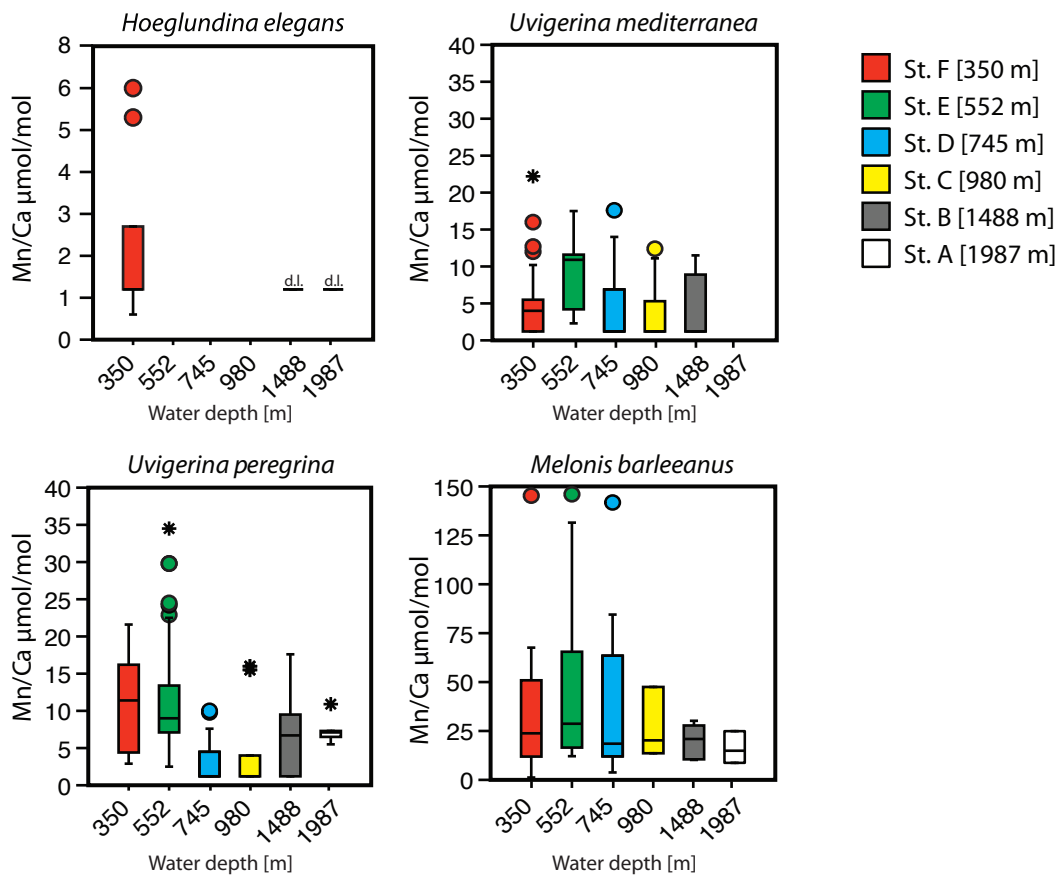
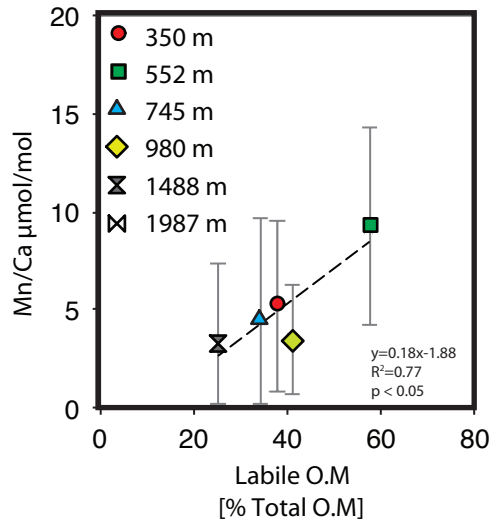
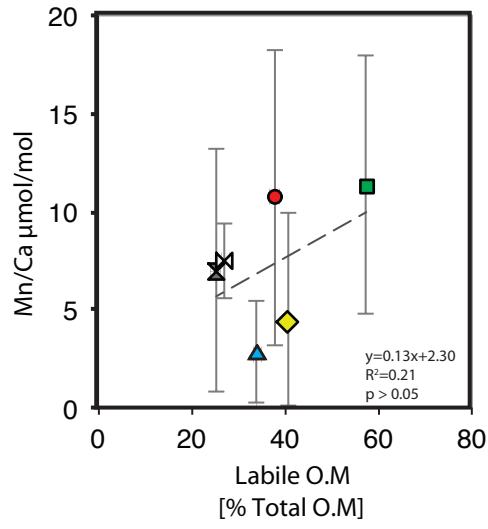


Figure 6. Box plots describing the distribution of Mn/Ca values across a depth transect (350-1987 m) measured in living (stained) individuals of *Hoeglundina elegans*, *Uvigerina mediterranea*, *Uvigerina peregrina* and *Melonis barleeanus*. Note that the scale of the y-axis varies. The box represents all values between the 25th and 75th percentile with the whiskers extending less than 1.5 times the box height. The dissection line through the box denotes the median. Values outside the whiskers are shown as circles, values further than 3 times the box height are denoted as stars.

Uvigerina mediterranea



Uvigerina peregrina



Melonis barleeanus

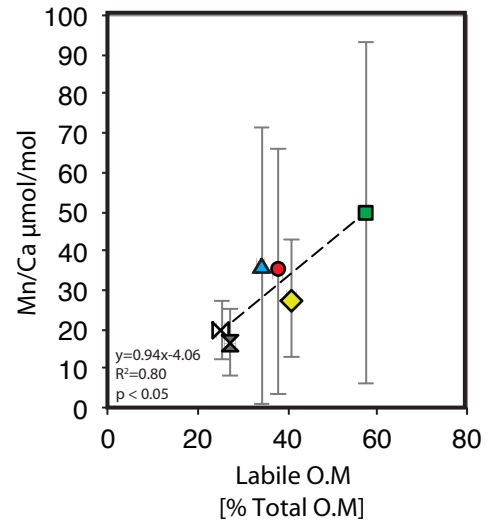


Figure 7. Plots of average Mn/Ca μmol/mol versus labile organic matter [% Total Organic matter].

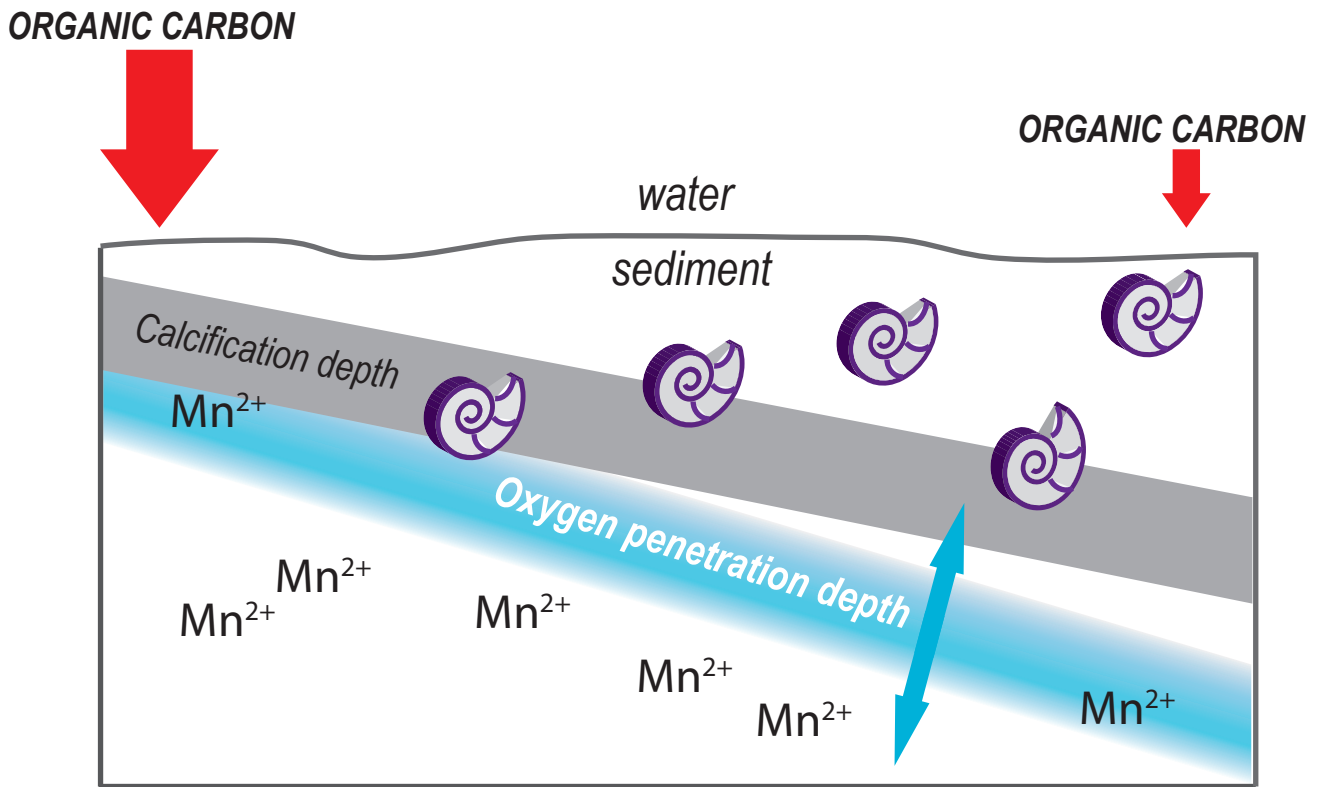


Figure 8. Schematic diagram of a shallow-inafaunal and intermediate-inafaunal benthic foraminifera and their spatial relationship with the sediment redox boundaries, migration zone, ALD and calcification depth.

Table 1. Water depth, coordinates and bottom water physio-chemical parameters: Temperature (°C), salinity, and oxygen penetration depth (mm) for six stations F-A. (* Xavier Durrieu de Madron, Pers. Comm.)

Station	Depth (m)	Latitude (N)	Longitude (E)	Bottom water temperature* (°C)	Bottom water salinity *	Oxygen penetration depth (mm)
F	350	42°52'32	4°42'43	13.2	~38.5	20.5 ±3.3
E	552	42°48'78	4°43'21	13.2	~38.5	57.2 ±4.5
D	745	42°46'66	4°43'91	13.1	~38.5	36.5 ±1.6
C	980	42°43'18	4°46'58	13.1	~38.48	50.7 ±6.3
B	1488	42°38'83	4°56'03	13.1	~38.46	141.5 ±0.0
A	1987	42°28'25	5°00'61	13.1	~38.46	197.0 ±11.0

Table 2. Number of LA-ICP-MS analyses per benthic foraminifera species per sample per station.

Station	Depth (m)	Sample intervals (cm)	<i>Hoeglundina elegans</i> no. analyses	<i>Uvigerina mediterranea</i> no. analyses	<i>Uvigerina peregrina</i> no. analyses	<i>Melonis barleeanus</i> no. analyses
F	350	0-0.5	2	18	5	1
		0.5-1	4	13		2
		1-1.5		3		
		1.5-2				10
		2-2.5	1			2
		3-3.5				3
		5-6				3
E	552	0-0.5		5	26	
		0.5-1			9	4
		1-1.5			14	3
		1.5-2			5	3
		2-2.5			7	3
		2.5-3			6	2
		3-3.5			6	
		3.5-4			8	1
		4-5		3		
7-8					1	
D	745	0-0.5		20	13	
		0.5-1		6		5
		1-1.5		3	6	
		1.5-2		7	8	6
		2-2.5			4	
		3.5-4			2	
		4-5			2	4
		8-9			2	
C	980	0-0.5		20		2
		0.5-1		20		2
		1-1.5		4		
B	1488	0-0.5	3	4	10	4
		0.5-1	9	5	3	5
A	1987	0-0.5	15		10	
		1-1.5				3

Table 3. Descriptive statistics (minimum, maximum, mean, median, standard deviation and interval of maximum frequency of total analyses for *H. elegans*, *U. mediterranea*, *U. peregrina* and *M. barleeanus* for Mn/Ca $\mu\text{mol/mol}$.

Mn/Ca $\mu\text{mol/mol}$	<i>H. elegans</i>	<i>U. mediterranea</i>	<i>U. peregrina</i>	<i>M. barleeanus</i>
Min	dl*	dl*	dl*	3.91
Max	0.69	22.71	35.38	149.50
Mean	0.04	4.03	8.28	37.22
Median	dl*	1.04	7.45	24.76
Std. deviation	0.16	5.03	7.17	35.17
Max. frequency interval	dl-7.50 (100% < 1)	dl-7.50 (80%)	dl-7.50 (53%)	7.5-15 (23%)

Table 4. Relative standard deviation (% RSD) of intra-individual values in Mn/Ca within four species of benthic foraminifera (*H. elegans*, *U. mediterranea*, *U. peregrina* and *M. barleeanus*).

Element	<i>H. elegans</i> % RSD	<i>U. mediterranea</i> % RSD	<i>U. peregrina</i> % RSD	<i>M. barleeanus</i> % RSD
Mn	21	23	20	51

Table 5. Relative standard deviation (% RSD) of inter-individual values in Mn/Ca within four species of benthic foraminifera (*H. elegans*, *U. mediterranea*, *U. peregrina* and *M. barleeanus*).

Element	<i>H. elegans</i> % RSD	<i>U. mediterranea</i> % RSD	<i>U. peregrina</i> % RSD	<i>M. barleeanus</i> % RSD
Mn	400	125	87	97

Table 6. Manganese porewater – carbonate partition coefficient for foraminiferal species *Uvigerina mediterranea*, *Uvigerina peregrina* and *Melonis barleeanus*.

Station	Partition coefficient (D) ¹		
	<i>U. mediterranea</i>	<i>U. peregrina</i>	<i>M. barleeanus</i>
E (552 m)	1.7	1.8	7.0
C (980 m)	1.2	-	5.1
B (1488 m)	2.2	2.3	4.1

¹Porewater-carbonate partition coefficients were calculated using the average porewater Mn/Ca [$\mu\text{mol/mol}$] measured above the oxygen penetration depth and the average carbonate Mn/Ca [$\mu\text{mol/mol}$] measured in *U. mediterranea*, *U. peregrina* and *M. barleeanus*, for all specimens recovered above the reported oxygen penetration depth (Fontanier et al., 2008).